[Article ID] 1003- 6326(2002)03- 0437- 04

Evolution of solid-liquid interface morphology of primary TiB_2 in non-equilibrium solidified Ti-Al-B alloys①

ZHANG Hu(张 虎)[1], GAO Wen-li(高文理)[2], JIN Yun-xue(金云学)[2], ZENG Song-yan(曾松岩)[2]
(1. School of Materials Science and Engineering, Beijing University of Aeronautics and Astronautics, Beijing 100083, China;
2. School of Materials Science and Engineering, Harbin Institute of Technology, Harbin 150001, China)

[Abstract] Ti-Al-B alloys were produced by in-situ synthesis method. The phase constitutions, microstructure of these alloys and the morphology of the primary TiB_2 were investigated by XRD and SEM. The results show that these alloys are composed of TiAl and TiB_2, and the primary TiB_2 is hexagonal prism shape. Growth terraces, pyramidal protrusion, and rod shape dendrites are observed on (0001) plane of primary TiB_2. There are thin flake convexes on plane of primary TiB_2, parallel to (0001) plane of the primary TiB_2. The rod-shaped crystal orientation and thin flake convexes are parallel to primary TiB_2 where they protrude out. The solid-liquid interface morphology of primary TiB_2 during solidification was also investigated. It was indicated that the solid-liquid interface morphology of primary TiB_2 is instable and gradually develops into a complicated interface consisted of a few separated secondary interfaces. These secondary interfaces are facet with the same crystalline orientation.

[Key words] TiAl; TiB_2; titanium alloys; crystal growth
[CLC number] TB331; TG115 [Document code] A

1 INTRODUCTION

TiAl alloys possess high specific strength, specific modulus and good oxidation resistance. They have been investigated as future candidate materials for aerospace and automobile engines and as replaced materials of current super-alloys[1~7]. According to continuous medium theory, the high-temperature strength of TiAl alloys can be improved by addition of second phase particles hampering the plastic flowing of matrix. However, the selected reinforcements must be thermodynamically stable and compatible with the matrix, and with a bigger size than that of dislocation cell. This kind of reinforcements can be achieved by incorporating ceramic phase forming elements, such as B, C, and solidification processing[8~12]. The reinforcements precipitates from molten metal and their morphology, size, and distribution depend on their crystal characteristics, solid-liquid interface morphology and growth conditions.

In present study, TiB_2 particles reinforced TiAl alloys are fabricated using in-situ synthesis method. The solid-liquid interface morphology of primary TiB_2, and its evolution and influence on the primary TiB_2 growth process are analyzed.

2 EXPERIMENTAL

Ti (99.2%, 45 μm), Al (99.6%, 29 μm) and B (99.8%, 45 μm) powders were mixed and dry ball milled for 24 h. Then they were pressed into prefabrication compacts and heated in vacuum to synthesize Al/TiB_2 master alloy. The Al/TiB_2 master alloy mixing with sponge Ti and high pure Al were melted in an arc-melter with a non-consumable tungsten electrode. Electron magnetic agitation was used and the ingots of 50 g were re-melted at least three times. Compositions of the samples used are Ti-50Al-1.2B (mole fraction, %), Ti-50Al-1.4B (mole fraction, %), Ti-54Al-1.4B (mole fraction, %) and Ti-54Al-1.7B (mole fraction, %), respectively. Phase analysis was carried out in a Rikagu D/max-RB X-ray diffractometer. Microstructures were observed on a Phillips S-570 scanning electron microscopy.

3 RESULTS AND ANALYSES

3.1 Microstructures

Fig. 1 shows the XRD pattern of as-cast Ti-50Al-1.2B alloy. This alloy consists of TiAl, Ti_3Al, and TiB_2. As shown in Fig. 2(a), coarse and blocky TiB_2 mainly distribute in matrix and fine flake, plate and bar shape TiB_2 locate at grain boundaries. Primary TiB_2 is hexahedral prism. The observed results are in agreement with the results in relevant Ref. [11]. Fig. 2(b) shows the growth terrace on (0001) plane of primary TiB_2.

Fig. 3 shows the magnified SEM photographs of primary TiB_2. It can be seen that on the (0001) plane of primary TiB_2 crystal, there exists convexes and rod-like branches which parallel to each other and perpendicular to (0001) plane. Their crystal orienta-

① [Received date] 2001- 07- 24; [Accepted date] 2002- 01- 10

tion is parallel to the crystal orientation of primary TiB_2 where they protrude out. Meantime, there also have thin flake convexes on plane of primary TiB_2, which parallel to each other and to (0001) plane of primary TiB_2. As observed in Fig. 3, the thickness of convex is less than 0.2 μm and the convex has the same crystal orientation as primary TiB_2.

3.2 Solidification and precipitation processing of primary TiB_2

In terms of Fig. 4, liquidus projection of Ti rich corner of Ti-Al-B system, TiB_2 is the primary phase during the solidification of Ti-50Al-(1.2, 1.4)B and Ti-54Al-(1.4, 1.7)B alloys. With the precipitation of TiB_2, in contrast to the decreasing of B concentration in molten metal, Al concentration increases.

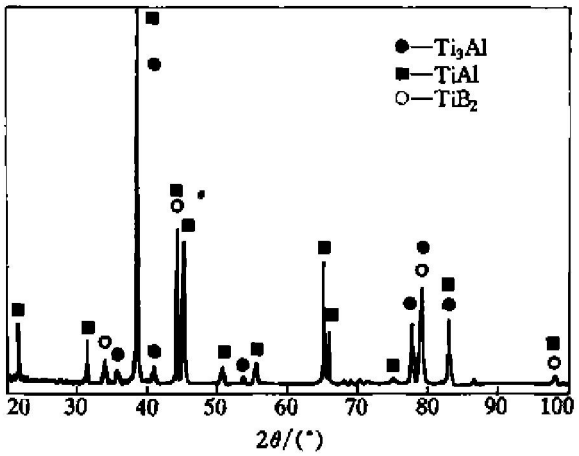

Fig. 1 XRD pattern of as-cast Ti-50Al-1.2B (mole fraction, %) alloy

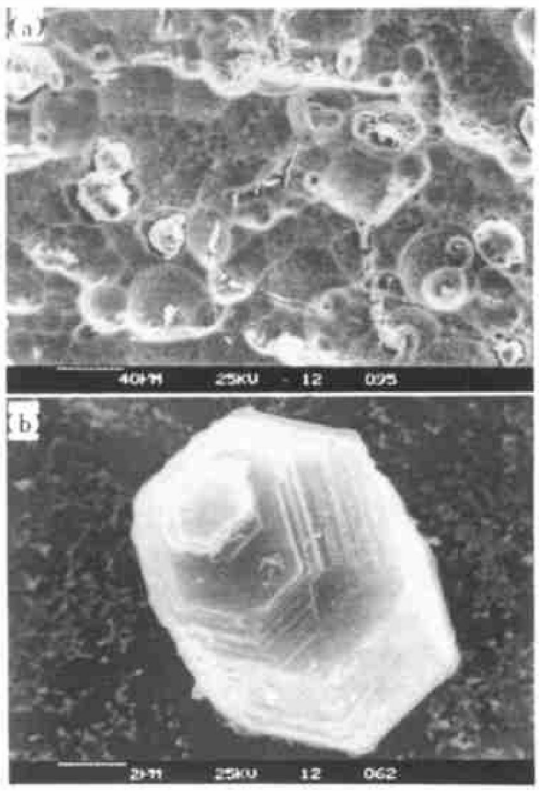

Fig. 2 Microstructures of TiAlB alloy
(a) —Dispersion of TiB_2 in matrix; (b) —Primary TiB_2

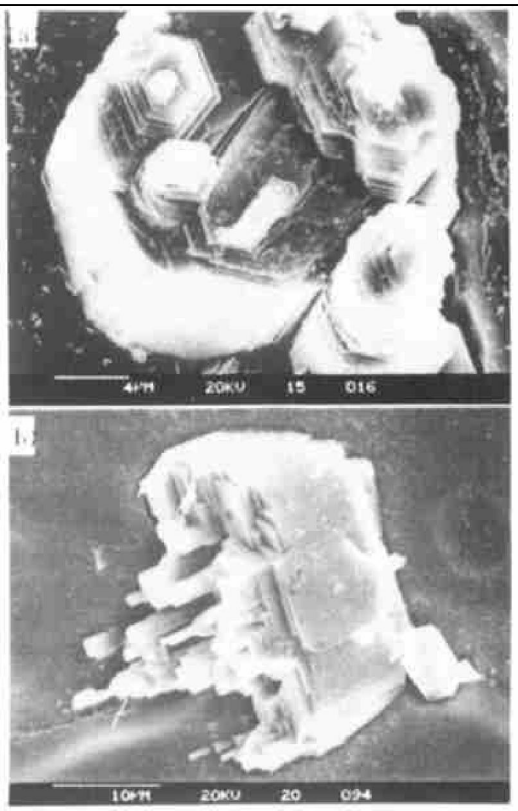

Fig. 3 Morphologies of primary TiB_2 in TiAlB alloy

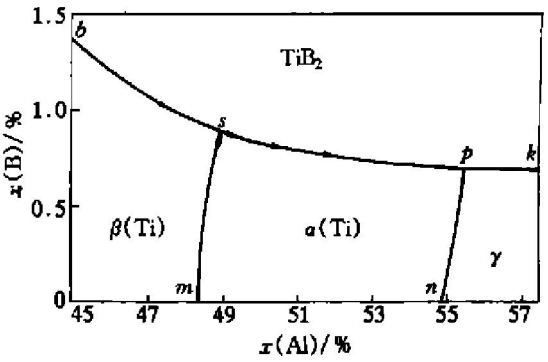

Fig. 4 Preliminary liquidus projection on titanium-rich side of Ti-Al-B ternary diagram

Molten constitution changes and it finally intersect with *b-s-p-k* line, then $L \rightarrow \alpha + TiB_2$ or $L \rightarrow \gamma + TiB_2$ reaction occurs. Under this experimental condition, TiB_2 grows in a liquid with lower B content and relatively higher Ti and Al content. Meantime, thermal diffusion coefficient is much more greater than solute diffusion coefficient. So, during the growth of primary TiB_2, Ti and Al elements are repelled to the front of the solid-liquid interface. In addition, Ti clusters in eutectic α or γ phases, and with the growth of TiB_2, Al rich boundary layer occurs in the front of the solid-liquid interface of TiB_2. On the other side, with the growth of TiB_2, the inhomogeneity of supersaturated B atoms at solid-liquid interface increases. TiB_2 can grow quickly at the location with higher supersaturated B atoms and protrude from Al rich boundary layer into liquid having higher B concentration, which leads to the quick growth of protruding TiB_2 and interface instability. Thus, TiB_2 crystal

protruding from Al rich boundary layer has higher growth rate. The growth direction of protruding TiB_2 is perpendicular to the solid-liquid interface.

3.3 Evolution of solid-liquid interface morphology of primary TiB_2 during solidification

Fig. 5 is the schematic for non-steady state growth of solid-liquid interface of primary TiB_2 crystal on [0001] and [$10\bar{1}0$] direction. According to analysis mentioned above, on (0001) plane of primary TiB_2, the protrusions have relatively higher growth rate along [0001] direction than the growth rate along [$10\bar{1}0$] direction. Lastly, they grow to rod-like convex and have the same crystal orientation with primary TiB_2 crystal. Furthermore, the protrusions on {$10\bar{1}0$} plane of primary TiB_2 crystal have relatively higher growth rate along [$10\bar{1}0$] direction than the growth rate along [0001] direction, and they become thin flake convex and also have the same crystal orientation with primary TiB_2. So, non-equilibrium solidification makes the solid-liquid interface morphology of primary TiB_2 changed.

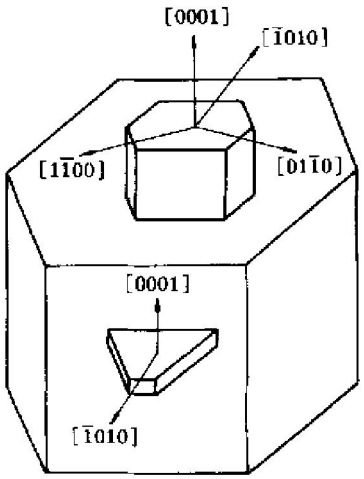

Fig. 5 Schematic of varying crystal-liquid interface of primary TiB_2 crystal on [0001] and [$10\bar{1}0$] direction

Fig. 6 shows the SEM photographs of deep

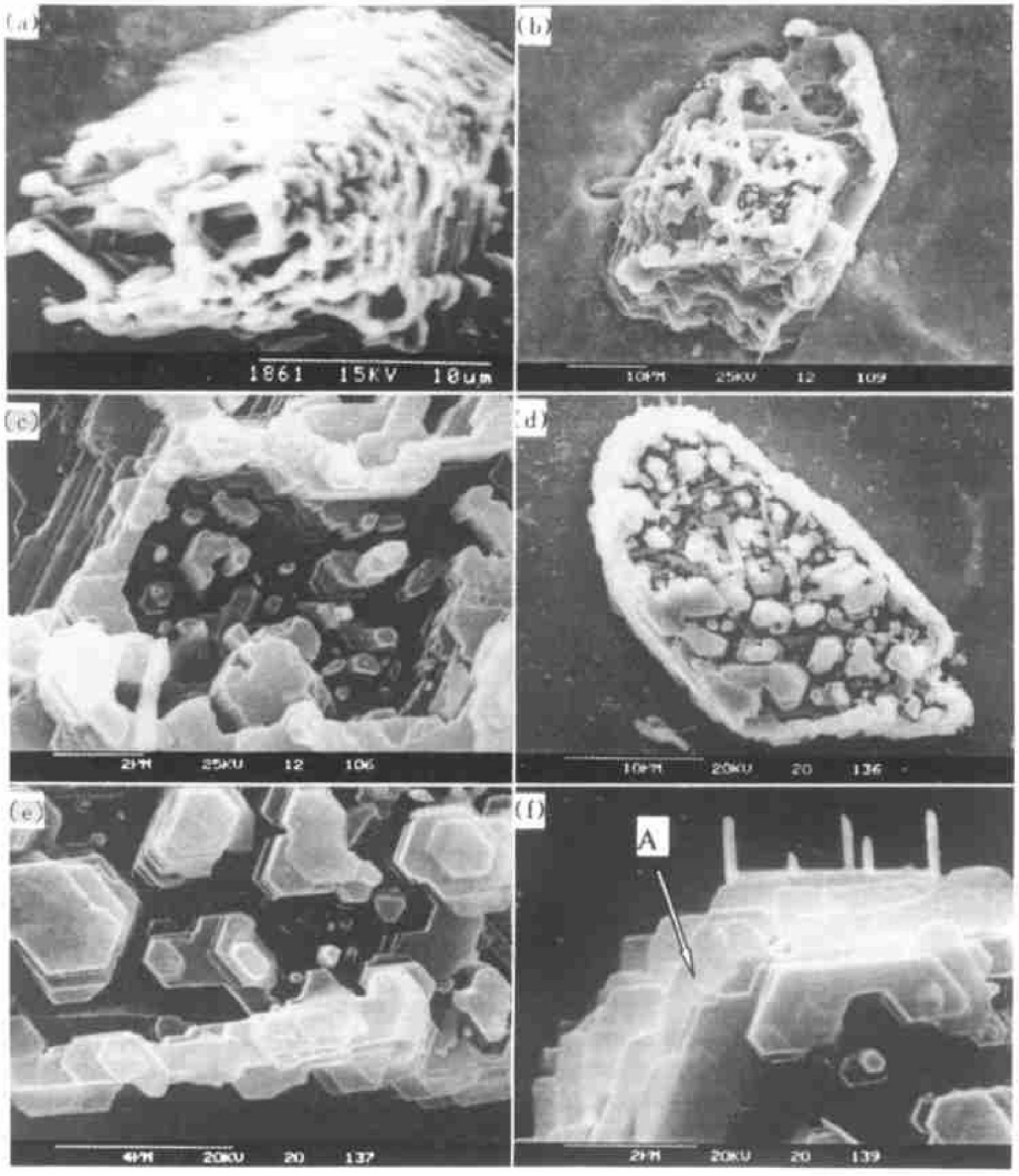

Fig. 6 Surface morphologies of primary TiB_2 crystal on (0001) facet
(a) —Hexagonal web; (b), (c) —Convex; (d), (e) —Convex branch; (f) —Thin flake

etched samples, show the solid-liquid interface morphology of primary TiB_2 crystal during the last stage of solidification. At the initial stage of non-steady state growth of solid-liquid interface, the solid-liquid interface morphology is hexagonal web shape which was caused by the incomplete separation of protrusions protruding from Al rich boundary layer in the front of solid-liquid interface, as shown in Fig. 6(a). In the middle stage of non-steady state growth of solid-liquid interface of primary TiB_2, interface instability increases resulting in partial separation of hexagonal web structure and forming convex structure (Fig. 6(b) and (c)). In the end, at the final stage of non-steady state growth of solid-liquid interface of primary TiB_2, interface instability further increases and solid-liquid interface divides into numerous secondary interfaces with facet characteristics. And more, there are numerous convex branches on (0001) plane of primary TiB_2. During the continuous growth, these convex branches compete to each other due to the existing of Al rich boundary layer. Among them, the convexes with higher growth rate will suppress the growth of neighboring convexes leading to the number of convexes decreases and the size of convexes increases. Primary TiB_2 crystal easily grows to be the morphology as shown in Fig. 3.

As mentioned above, the solid-liquid interface of primary TiB_2 is also instable in $[10\bar{1}0]$ direction and evolves into numerous thin flakes from a big interface. These thin flakes grow with higher rate in $[10\bar{1}0]$ direction than in [0001] direction. Thus, these thin flakes remain thin flake shape and the solid-liquid interface also remains its original morphology. On plane of primary TiB_2, the thickness of thin flake is less than 0.2 μm and the length of thin flake protruding from master TiB_2 is less than 1.5 μm as a arrowhead showing in Fig. 6(f).

4 CONCLUSIONS

1) On the $\{10\bar{1}0\}$ plane of primary TiB_2, there are thin convexes parallel to each other along (0001) plane. Also, there are rod-like branches on (0001) plane of primary TiB_2 parallel to [0001] crystal direction of primary TiB_2. In the meantime, these thin convex and rod-like branches possess the same orientations as their master TiB_2.

2) During solidification of Ti-Al-B alloys, the integrative and smooth solid-liquid interface gradually changed into a few separated secondary interfaces. These secondary interfaces are facet with the same orientation as their original one.

3) Under the non-equilibrium solidification conditions, the Al rich boundary layer in the front of primary TiB_2 and the increasing inhomogeneity of the supersaturated B atoms at the solid-liquid interface due to the growth of TiB_2 lead to non-steady state growth of solid-liquid interface of the primary TiB_2, which resulting in the change of the solid-liquid interface morphology and the evolution of the primary TiB_2 morphology.

[REFERENCES]

[1] Valencia J J, Lǒfvander J P A, McCullough C, et al. In-situ-grown reinforcements for titanium aluminides [J]. Materials Science and Engineering, 1991, A144: 25-36.

[2] ZHANG Hu, ZHANG Er-lin, GAO Wen-li, et al. Microstructure of Ti-40Al-2B alloy and growth characteristics of primary TiB_2 [J]. Acta Materiae Compositae Sinica, 2001, 18(4): 46-49.

[3] ZHOU Ke-chao, HUANG Bai-yun, QU Xuan-hui, et al. Fine microstructure and fracture toughness of Ti-Al based alloys [J]. The Chinese Journal of Nonferrous Metals, (in Chinese), 1996, 6: 111-114.

[4] CHEN Shi-qi, QU Xuan-hui, LEI Chang-ming, et al. Effect of rare earths addition on microstructure and mechanical property of cast TiAl-base alloys [J]. The Chinese Journal of Nonferrous Metals, (in Chinese), 1995, 5: 63-67.

[5] Saqib M, Weiss I, Mehrotra G M, et al. Microstructural and thermal stability of a Ti-43Al alloy containing dispersoids of titanium Di-boride [J]. Metall Trans A, 1991, 22A: 1721-1728.

[6] ZHANG Hu, GAO Wen-li, ZHANG Er-lin, et al. Growth mechanism of primary hollow TiB in Ti-Al-B alloy [J]. Acta Materiae Compositae Sinica, 2001, 18(4): 50-53.

[7] ZHANG Hu, GAO Wen-li, HE Jian-pin, et al. Effect of B content on the morphology of TiB_2 in Ti-50Al-xB [J]. J Materials Engineering, 2001(12): 36-39.

[8] ZHANG Er-lin, ZENG Song-yan. Microstructure of in-situ TiC particulate titanium matrix composites [J]. Trans Nonferrous Metals Soc China, 2000, 10: 764-768.

[9] Lu L, Lai M O, Wang H Y. Synthesis of titanium di-boride TiB_2 and Ti-Al-B metal matrix composites [J]. J Mater Sci, 2000, 35: 241-248.

[10] Hashimoto Hitoshi, Sato Hitraku, Abe Toshihiko. Synthesis of TiAl-TiB_2 composites material by mechanical alloying and spark plasma activated sintering [J]. Journal of the Japan Society of Powder and Powder Metallurgy, 1996, 43(3): 289-294.

[11] Abdel-Hamid A A, Hamar Thibault S, Hamar R. Crystal morphology of the compound TiB_2 [J]. Journal of Crystal Growth, 1985, 71: 744-750.

[12] Hyman M E, McCullough C, Valencial J J, et al. Microstructure evolution in TiAl alloys with B addition: conventional solidification [J]. Metall Trans A, 1989, 20A: 1847-1859.

(Edited by HUANG Jin-song)